De novo biosynthesis of the hops bioactive flavonoid xanthohumol in yeast

Shan Yang
Dalian Institute of Chemical Physics
Ruibing Chen
Dalian Institute of Chemical Physics https://orcid.org/0000-0002-7933-3670
Xuan Cao
Dalian Institute of Chemical Physics
Guodong Wang
Institute of Genetics and Developmental Biology https://orcid.org/0000-0001-9917-0656
Yongjin zhou (zhouyongjin@dicp.ac.cn)
Dalian Institute of Chemical Physics https://orcid.org/0000-0002-2369-3079

Article

Keywords:

Posted Date: June 2nd, 2023

DOI: https://doi.org/10.21203/rs.3.rs-2923518/v1

Additional Declarations: There is **NO** Competing Interest.

De novo biosynthesis of the hops bioactive flavonoid xanthohumol in yeast

Shan Yang[1, 2], Ruibing Chen[1], Xuan Cao[1], Guodong Wang[3], Yongjin J. Zhou [1, 4, 5]

[1]Division of Biotechnology, Dalian Institute of Chemical Physics, Chinese Academy of Sciences, Dalian, 116023, China

[2]University of Chinese Academy of Sciences, Beijing, 100049, China

[3]State Key Laboratory of Plant Genomics, Institute of Genetics and Developmental Biology, The Innovative Academy of Seed Design, Chinese Academy of Sciences, Beijing 100101, China

[4]CAS Key Laboratory of Separation Science for Analytical Chemistry, Dalian Institute of Chemical Physics, Chinese Academy of Sciences, Dalian, 116023, China

[5]Dalian Key Laboratory of Energy Biotechnology, Dalian Institute of Chemical Physics, Chinese Academy of Sciences, Dalian, 116023, China

Abstract

The flavonoid xanthohumol is an important flavor substance in the brewing industry that has a wide variety of bioactivities. However, its unstable structure is easily oxidized during the brewing process, resulting in its low content in beer. Moreover, its extraction and purification from plants requires laborious and expensive procedures. Microbial biosynthesis is considered a sustainable and economically viable alternative to supply natural products. However, the complex structures of natural products and regulation of the biosynthetic pathways make it challenging to construct and optimize the xanthohumol pathway in microbes. Here, we harnessed the brewing yeast *Saccharomyces cerevisiae* for the *de novo* biosynthesis of xanthohumol from glucose by modular fine-tuning of the competitive metabolic pathways, prenyltransferase engineering, enhancing precursor supply, substrate channeling, and peroxisomal engineering. These strategies significantly improved the production of the key xanthohumol precursor demethylxanthohumol (DMX) by 83-fold and achieved the *de novo* biosynthesis of xanthohumol for the first time in a microbial cell factory. We also revealed that prenylation is the key limiting step in DMX biosynthesis and that enhancing the supply of dimethylallyl pyrophosphate (DMAPP) and substrate channeling helps to drive the metabolic flux toward DMX biosynthesis, which should be helpful for improving the production of prenylated natural products. Our work provides feasible approaches for systematically engineering yeast cell factories for the *de novo* biosynthesis of complex natural products.

Introduction

Hops (*Humulus lupulus* L., Cannabaceae), an essential ingredient in beer brewing, contain many secondary metabolites, including essential oils, bitter acids and prenylated flavonoids[1, 2]. Among these metabolites, xanthohumol is a prenylated flavonoid that has a variety of biological activities, such as the prevention of cancer, the prevention and mitigation of diabetes, and antioxidant, anti-inflammatory, antibacterial and immunomodulatory effects[3-7]. However, the low concentration (0.1-1% dry cell weight) and instability of xanthohumol during beer brewing do not allow the pharmacological and health effects of xanthohumol to be obtained through beer ingestion [8]. Furthermore, xanthohumol extraction from hops faces material shortages due to geographical limitations, and the leftover solid waste [9] and solvent use[10, 11] will bring environmental stress.

Alternatively, microbial biosynthesis provides a versatile approach for the sustainable production of scarce natural products due to the great developments in metabolic engineering and synthetic biology[12, 13]. The brewing yeast *Saccharomyces cerevisiae* is considered an ideal host for the production of phyto-natural products, including terpenoids, alkaloids and flavonoids[14-16]. Thus, engineering *S. cerevisiae* for such biosyntheses might provide a sustainable route to supply large amounts of xanthohumol for nutraceutical applications and enhance the xanthohumol level in beer, since engineering monoterpene biosynthesis in brewing yeast gives rise to a hoppy beer flavor[17]. The complexity of biosynthetic pathways and the tight regulation of precursor supply make it challenging to reconstruct the *de novo* biosynthesis of xanthohumol in yeast cell factories. Indeed, have not yet been any reports on microbial xanthohumol biosynthesis. This is true even though Canada initiated the PhytoMetaSyn project to engineer yeast to biosynthesizesix plant natural products (three isoprenoids, two alkaloids and xanthohumol) based on their potential commercial markets[18], and succeeded in the microbial biosynthesis of five compounds, including the benzylisoquinoline alkaloid morphine[19] and the monoterpenoid indole alkaloid strictosidine[20], in the last few years.

In recent decades, considerable efforts have been made to identify the key enzymes in the complete biosynthetic pathway of xanthohumol[2, 21-24]. To facilitate the construction and optimization of xanthohumol biosynthesis in yeast, we modularly mapped the biosynthetic pathway from glucose, which comprises four modules: *p*-coumaric-CoA (*p*-CA-CoA) biosynthesis (Module I), malonyl-CoA supply (Module II), prenylation (Module III) and methylation (Module IV) (Fig. 1). The parallel biosynthesis of the three precursors, *p*-CA-CoA, malonyl-CoA and dimethylallyl pyrophosphate (DMAPP), requires careful balancing and tuning of the biosynthetic pathways and is distinct from common upstream to downstream pathways, such as terpenoid biosynthesis (Supplementary Fig. 1) [25].

In this work, we extensively engineered a yeast platform for the *de novo* biosynthesis of xanthohumol by developing a modular metabolic engineering strategy. We first enhanced the supply of precursors *p*-CA-CoA, malonyl-CoA and DMAPP by balancing the three parallel aromatic biosynthesis, malonyl-CoA supply, and the mevalonate (MVA) pathway. We then enhanced the limiting prenylation step by selecting and engineering prenyltransferase (PTase), and enhancing the DMAPP supply and substrate channeling, which enabled the production of 4.0 mg/L demethylxanthohumol (DMX), which is an 83-fold improvement compared with the starting strain. We also tried to compartmentalize a partial DMX synthesis pathway into peroxisomes to avoid crosstalk with competing cytosolic pathways. Finally, optimization of the last methylation step achieved the *de novo* biosynthesis of xanthohumol from glucose in yeast. This first microbial biosynthesis of xanthohumol will allow microbial cell factories to be optimized for the sustainable supply of xanthohumol and provide feasible approaches to optimize other complex biosynthetic pathways of natural products.

Results

Modular construction of the xanthohumol biosynthetic pathway

First, we modularly constructed the biosynthetic pathway to produce DMX, the key precursor of xanthohumol. We first constructed the downstream pathway of DMX

biosynthesis starting with L-tyrosine by expressing the tyrosine ammonia-lyase gene *FjTAL* from *Flavobacterium johnsoniae*[26], the 4-coumarate-coenzyme A ligase gene *HlCCL1*[2], the chalcone synthase gene *CHS_H1*[22] and the prenyltransferase gene *HlPT1L*[24] from *H. lupulus* (Fig. 2a). We also expressed a noncatalytic chalcone isomerase gene, *HlCHIL2*, from *H. lupulus*, which has been shown to enhance the activities of CHS_H1 and HlPT1L[21]. In addition, the *H. lupulus O*-methyltransferase gene *HlOMT1*[23] was expressed to examine the possible xanthohumol production from DMX. The resulting strain YS103 produced 25 mg/L naringenin chalcone (NC) and naringenin (N, a product spontaneously formed product from the unstable compound NC[27]), but neither xanthohumol nor DMX (Fig. 2b, d).

We then tried to optimize the upstream biosynthetic pathway to enhance the synthesis of the precursors L-tyrosine, malonyl-CoA and DMAPP. We first tried to enhance L-tyrosine biosynthesis by knocking out *ARO10*, which encodes the competing enzyme phenylpyruvate decarboxylase, as well as overexpressing $ARO4^{K229L}$ (encoding a feedback-inhibition resistant version of DAHP synthase) and $ARO7^{G141S}$ (encoding a chorismate mutase)[28]. The resulting strain YS107 produced 48% more NC/N than that of the parent strain YS103 (Fig. 2b). We then tried to improve malonyl-CoA biosynthesis by replacing the native promoter of the acetyl-CoA carboxylase gene (*ACC1*) with the constitutive promoter P_{TEF1}[29]. This replacement marginally improved the production of NC/N, suggesting that the malonyl-CoA supply was not currently a bottleneck.

Finally, we attempted to enhance prenylation step by enhancing the supply of the low-level substrate DMAPP and overexpressing of the PTase gene. Overexpressing the MVA rate-limiting genes *tHMG1* (truncated HMG-CoA reductase 1) and *IDI1* (isopentenyl diphosphate isomerase) still failed to produce DMX in strain YS112. We speculated that the efficient process of farnesyl diphosphate (FPP) biosynthesis competed with the biosynthesis with DMAPP, and it has been reported that the FPP synthase mutation $ERG20^{N127W}$ resulted in decreased activity in catalyzing DMAPP turnover[30]. Thus, we mutated *ERG20 in situ* to $ERG20^{N127W}$ to improve the DMAPP

accumulation, which succeeded in producing 13 μg/L DMX in strain YS116 (Fig. 2c, d). Interestingly, this modification improved NC/N production by 79% (Fig. 2b), which might be due to driving the metabolic flux toward L-tyrosine and malonyl-CoA from the downregulation of FPP biosynthesis. Subsequently, we attempted to overexpress *HlPT1L* by using a high-copy plasmid, and the resulting strain YS117 produced 7.3-fold more DMX (104 μg/L) than the parent strain YS116 (Fig. 2c, d), which indicated that PTase was a limiting factor in DMX production.

Characterizing and engineering PTase

We further tried to enhance PTase activity to improve DMX production (Fig. 3a). It has been reported that membrane PTase is targeted to plastids with a high pH in plants[22], while the yeast cytosolic pH is low (< 6) due to the accumulation of acidic metabolites[31]. Therefore, we cultivated the engineered *S. cerevisiae* YS116 with MES buffered media, which maintained the pH of the media at 5.4 for 48 h of cultivation, while the pH of the control media was 3.3. The DMX production in the buffered medium was 2.8-fold higher than that in the nonbuffered medium (Fig. 3b). However, there was complete transformation of the precursor NC into N, indicating that the high pH in the cytosol made it difficult to stabilize the ring-opened conformation of NC (Fig. 3b).

We then searched for alternative PTases from hops and other organisms based on similarities of the substrate flavonoids and prenyl donors, including hops HlPT-1[32] with 98.5% homology to HlPT1L, four chalcone-specific PTases that catalyze the condensation of isoliquiritigenin and DMAPP (MaIDT[33] and CtIDT[33] from the Moraceae family and GuILDT[34] and SfiLDT[35] from the Leguminosae family), four isoflavone-specific PTases (SfFPT[36], LaPT1[37], AhR4DT-1[38] and PcM4DT[39]), *Cannabis sativa L.* CsPT3[40] and CsPT4[41], and a soluble PTase NphB[42] from *Streptomyces sp.* An overview of all examined PTases and their substrate specificities are presented in Supplemental Table S1. Amino acid sequence alignment of these 13 PTases was performed to construct a phylogenetic tree and to evaluate the evolutionary relationship between HlPT1L and these other PTases (Fig. 3c). The results showed that HlPT1L and CsPT4 were in the same branch, indicating that their enzymatic catalytic functions were

similar. HlPT1L was also closely evolutionarily related to MaIDT, CtIDT and CsPT3 but was far removed from other PTase enzymes.

We expressed these 12 codon-optimized PTases and HlPT1L in strain YS116 by using a high-copy plasmid (Fig. 3d). When MaIDT, HlPT-1 and LaPT1 were expressed, significantly more DMX was produced than when HlPT1L was expressed, among which LaPT1 led to the highest DMX production of 121 μg/L (Fig. 3d). We then truncated the N-terminal signal peptide to improve the enzyme activity with the aid of the signal peptide prediction software TargetP (https://services.healthtech.dtu.dk/services/TargetP-2.0/), and the truncated sequence positions are shown in Supplementary Fig. 2. Subsequently, the truncated PTase sequences, together with the full-length sequences, were transferred into strain YS116 to evaluate DMX production. Truncation of HlPT1L, MaIDT and LaPT1 improved DMX production (Fig. 3e-g), while truncation of HlPT-1 led to lower DMX production than the original version (Fig. 3h). Finally, truncated *HlPT1L*$_{\Delta 1\text{-}83}$ was used for further experiments.

Pathway optimization to improve DMX biosynthesis

Next, we tried to optimize the biosynthetic pathways to improve precursor supply (Fig. 4a). We first optimized the MVA pathway to supply the precursor DMAPP. *ERG20*^{N127W} was downregulated to further decrease the turnover of DMAPP, by replacing its native promoter with the *HXT1* promoter[43] (strain YS119) or *ERG1* promoter[44] (strain YS120), and DMX production was improved by 2-fold and 1.4-fold than compared with the parent strain YS116, respectively (Fig. 4b). P_{HXT1} is a high glucose-induced and low glucose-repressed promoter that should be helpful when synchronizing DMX biosynthesis with the modified GAL regulation system[45]. We also overexpressed the *ERG10* gene encoding acetoacetyl-CoA thiolase and *HMG2*^{K6R} encoding a mutant of endogenous HMG-CoA reductase (strain YS121)[46], which improved DMX production by 1.9-fold compared to control strain YS116. The genome integrating another two copies of *HMG2*^{K6R} (strain YS123) further improved DMX production by 34% compared with strain YS121. These results indicated that overexpressing rate-limiting

genes in the MVA pathway could increase the supply of DMAPP, thereby increasing DMX production. However, we found that the amount of precursor NC/N in strain YS123 was slightly reduced compared with that in strain YS121 (Supplementary Fig. 3), indicating that continued overexpression of MVA pathway genes would lead to excessive metabolic flux into the MVA pathway, thus reducing amino acid biosynthesis. Therefore, we tried to construct an isopentenol utilization pathway (IUP)[47] to supply DMAPP by alleviating the metabolic stress on central carbon metabolism. However, expression of the IUP with isopentenol supplementation failed to improve DMX production and decreased the biosynthesis of precursor NC/N (Supplementary Fig. 4).

Since *p*-coumaric acid (*p*-CA) was not detected in the strain, we speculated that increasing the *p*-CA supply could further improve DMX production. Feeding different concentrations of *p*-CA was helpful to increase DMX production (Supplementary Fig. 5), among which feeding 280 mg/L *p*-CA at 24 h significantly improved DMX production by 1.8-fold (Fig. 4d). Interestingly, there was almost no *p*-CA remaining, suggesting that all of the *p*-CA was converted into *p*-CA-CoA. Therefore, we tried to enhance the turnover of *p*-CA-CoA toward NC biosynthesis by overexpressing *CHS_H1* and *HlCHIL2* in strain YS116. The resulting strain YS125 produced 2.1-fold and 1.8-fold more DMX and NC than the parent strain YS116 respectively (Fig. 4e), suggesting that overexpressing *CHS_H1* and *HlCHIL2* drives metabolic flux toward NC biosynthesis and DMX production.

Although an increase in the supply of DMAPP and NC significantly improved DMX production, the DMX titer was still low (< 150 μg/L). Considering that the presence of a signal peptide prevented the PTase enzyme from quickly contacting the substrates DMAPP and NC, we further expressed two extra copies of $HlPT1L_{\Delta 1\text{-}83}$, which improved DMX production to 180 μg/L in strain YSC1 (Fig. 4e). Unfortunately, the introduction of $HlPT1L_{\Delta 1\text{-}83}$ increased DMX production by only 21% compared to the strain YS125. We found that the total production of NC/N in strain YSC1 reached 155 mg/L, indicating that a there was sufficient amount of the precursor NC in the cytosol. At the same time, DMAPP was dynamically present in cells, as the accumulation of

DMAPP has been reported to be toxic to host cells[48, 49]. Furthermore, IDI1 catalyzes the isomerization of IPP into DMAPP. To help DMAPP quickly interact with PTase, we attempted to fuse IDI1 with HlPT1L$_{\Delta 1\text{-}83}$. Genomic integration of two copies of the fusion gene *IDI1-HlPT1L$_{\Delta 1\text{-}83}$* resulted in breakthrough DMX production of 4 mg/L in strain YSC3, which was 83-fold and 21-fold higher than that in strains YS116 and YSC1, respectively (Fig. 4e). These results showed that the IDI1-HlPT1L$_{\Delta 1\text{-}83}$ fusion protein strategy could indeed allow quick contact between DMAPP and the PTase enzyme and significantly improve the production of DMX. Due to the significant effect of this fusion strategy, we further transferred two extra copies of *IDI1-HlPT1L*$_{\Delta 1\text{-}83}$ into strain YSC3 to obtain strain YSC4 (Supplementary Fig. 6), hoping to further increase DMX production. Moreover, because HlCHIL2 could enhance the activity of the HlPT1L enzyme, we tried to fuse HlCHIL2 with HlPT1L$_{\Delta 1\text{-}83}$ to improve DMX production. Unfortunately, we found that the addition of these two fusion proteins significantly decreased DMX production by 74% (IDI1-HlPT1L$_{\Delta 1\text{-}83}$) and 65% (HlCHIL2-HlPT1L$_{\Delta 1\text{-}83}$), respectively, compared with strain YSC3 (Supplementary Fig. 6).

Peroxisome compartmentalization for DMX biosynthesis

We showed that channeling the substrate DMAPP was critical for the prenylation reaction during DMX biosynthesis. Sub-organelle compartmentalization is helpful for selective production, as it relieves the competition with cytosolic enzymes[50]. Peroxisomes are ideal compartments with an efficient supply of acetyl-CoA from fatty acid β-oxidation and the absence of fatty acid biosynthesis and FPP competition[51, 52], which might be helpful to accumulate the DMX precursors DMAPP and malonyl-CoA. We thus compartmentalized the DMX downstream pathway from *p*-CA into peroxisomes with reconstruction of the peroxisomal DMAPP biosynthetic pathways (Fig. 5a). We used a previously constructed *p*-CA-overproducing (131 mg/L) strain RB14 as a chassis[45] and then overexpressed *ARO1* (encoding shikimate dehydrogenase), *ARO2* (encoding chorismate synthase) and *ARO3* (encoding DAHP synthase) in strain RB14 to obtain strain RB99 to further improve *p*-CA production. Peroxisomal targeting of endogenous *ACC1* (*ACC1*$_{\text{per}}$) and exogenous *CHS_H1*$_{\text{per}}$ and *HlCCL1*$_{\text{per}}$ (strain

YS1per) resulted in 28 mg/L NC/N production (Fig. 5b). Further peroxisomal construction of prenylation through the expression of *IDI1*$_{per}$, *HlPT1L*$_{\Delta 1\text{-}86per}$ and *HlCHIL2*$_{per}$ failed to produceDMX in the engineered strain YS2per (Fig. 5b, c).

To provide a sufficient pool of the precursor DMAPP for DMX production, we reconstructed the MVA pathway in peroxisomes. We expressed *Enterococcus faecalis* *EfmvaE*$_{per}$ (bifunctional acetoacetyl-CoA thiolase/HMG-CoA reductase) and *EfmvaS*$_{per}$ (HMG-CoA synthase)[53] to catalyze the first three steps of the MVA pathway due to their high efficiency and absence of feedback regulation in yeast. *ERG12*$_{per}$, *ERG8*$_{per}$ and *ERG19*$_{per}$ were also expressed in peroxisomes; however, the engineered strain YS5per with the peroxisomal MVA pathway led to the production of a low DMX titer (6 μg/L). We then enhanced the prenylation step by adding another two copies of peroxisomal *HlPT1L*$_{\Delta 1\text{-}86per}$ (strain YS8per), which slightly improved DMX production (Fig. 5c). Subsequently, *CHS_H1*$_{per}$ and *HlCHIL2*$_{per}$ were expressed in strain YS8per, and the resulting strain YS9per produced 63% more DMX than the parent strain YS8per (Fig. 5c).

After enhancement of the prenylation step, we further tried to increase the DMAPP supply by expressing another two copies of the most essential gene *ERG12*$_{per}$[52] (strain YS11per), which improved DMX production by 94% (Fig. 5d). This significant improvement encouraged us to further optimize the peroxisomal MVA pathway. Thus, *ERG12*$_{per}$, *EfmvaE*$_{per}$ and *EfmvaS*$_{per}$ were overexpressed in a high-copy plasmid coexpressing *HlPT1L*$_{\Delta 1\text{-}86per}$, and the resulting strain YS12per produced 2.7-fold more DMX than strain YS9per (Fig. 5d). We also tried to express the fusion gene *IDI1-HlPT1L*$_{\Delta 1\text{-}86per}$ to channel DMAPP toward PTase (strain YS15per), which improved DMX production by 69% compared to strain YS9per. However, the DMX titers were still low (< 100 μg/L) and were much lower than those of the cytosolic pathway (4.0 mg/L in strain YSC3). This low DMX production might be attributed to the low activity of the PTase enzyme in peroxisomes.

Biosynthesis of xanthohumol

We finally tried to biosynthesize xanthohumol from DMX by expressing the *O*-methyltransferase gene *HlOMT1* from *H. lupulus* in the chassis YSC3 harboring the cytosolic DMX biosynthetic pathway (Fig. 6a). We expressed the original version of *HlOMT1* and codon-optimized version *HlOMT1*sc for expression in *S. cerevisiae* in the chassis strain YSC3. The resulting strains YSC6 (*HlOMT1*) and YSC7 (*HlOMT1*sc) produced 48 μg/L and 141 μg/L xanthohumol (Fig. 6b), respectively, and liquid chromatography-mass spectrometry analysis verified xanthohumol production (Supplementary Fig. 7). The high accumulation of DMX (1.1 mg/L-2.3 mg/L) suggests that the methylation step should be further enhanced for efficient xanthohumol production from DMX.

Discussion

Hops (*H. lupulus* L.) are valuable sources of several secondary metabolites, such as essential oils, bitter acids and flavonoids, which have potential medical applications. Microbial synthesis is considered a feasible approach for the efficient production of low-content natural products such as bitter acids and essential oils from hops[17, 54]. Xanthohumol is a functional flavonoid in beer that has a variety of pharmacological effects. However, its complex biosynthesis poseschallenges for its *de novo* production in microbes. In this study, we systematically engineered the budding yeast *S. cerevisiae* for *de novo* xanthohumol biosynthesis by optimizing the biosynthetic pathway and rewiring the cellular metabolism.

To facilitate pathway construction and optimization, we divided the reconstructed metabolism into three modules: the *p*-CA-CoA, malonyl-CoA and MVA biosynthetic pathways. Here, we identified that the prenylation of NC with DMAPP was a limiting step in the biosynthesis of DMX, the last precursor of xanthohumol. Thus, the prenylation step should be enhanced to improve DMX production. Here, we applied enzyme discovery, truncation of the signal peptide and enhancement of expression levels to improve PTase activity, which significantly improved DMX biosynthesis from NC.

In addition to PTase activity, the limited availability of DMAPP is another bottleneck for efficient prenylation[55, 56], since DMAPP is efficiently transformed toward FPP in ergosterol biosynthesis in yeast. To improve DMAPP availability, we reduced DMAPP consumption toward FPP by expressing an FPPS mutant gene *ERG20*^{N127W}, downregulating the expression of native *ERG20* and overexpressing key rate limiting MVA genes for enhanced upstream flux. These strategies considerably improved the DMX production; however, it was still lower than 0.1 mg/L. Interestingly, expressing *IDI1-HlPT1L*$_{\Delta 1\text{-}83}$, encoding a fusion enzyme of IPP isomerase and truncated PTase, significantly improved DMX production by 21-fold compared with when *HlPT1L*$_{\Delta 1\text{-}83}$ was expressed. This modification could not only increase the supply of DMAPP but also facilitate the channeling of DMAPP toward PTase with a shortened distance. Therefore, the key limitation for a higher product yield in our studies was the availability of the prenyl donor and colocalization of the substrates and PTase, as supported by the findings of several other studies on the production of prenylated compounds in yeast[41, 55-57]. In addition, the rate-limiting PTase can be modified by protein engineering to increase its selectivity to specific substrate donors[42, 58].

Finally, overexpressing the optimized *O*-methyltransferase gene *HlOMT1* achieved, for the first time to our knowledge, the *de novo* biosynthesis of xanthohumol in yeast. However, the low titer (0.14 mg/L) suggested that the activity of HlOMT1 and/or the recycling of SAM should be enhanced to improve the transformation of DMX to xanthohumol, since much more DMX remained in the engineered strain. Furthermore, xanthohumol biosynthesis involves parallel biosynthetic pathways for three precursors *p*-CA-CoA, malonyl-CoA and DMAPP, which is quite different from single-channel biosynthetic pathways such as terpenoid biosynthesis (Supplementary Fig. 1), and thus requires careful balancing of the parallel biosynthetic modules.

In summary, we systematically engineered yeast for the *de novo* microbial production of xanthohumol from the inexpensive carbon source glucose in a minimal medium by optimizing the metabolic flow of three modules.

Methods and Materials

Strains, plasmids, and reagents

Escherichia coli DH5α was used for plasmid construction and amplification. *S. cerevisiae* strain SY03 (*MATa*, *MAL2-8c*, *SUC2*, *his3Δ*, *ura3-52*, *gal80Δ*, *XI-5::*P_{TEF1}*-Cas9-*T_{CYC1}) derived from CEN.PK113-11C (*MATa*, *MAL2-8c*, *SUC2*, *his3Δ*, *ura3-52*) was used as the background strain for strain construction[59]. The flowchart of yeast strain construction is described in Supplementary Fig. 8. The detailed genotypes of the engineered strains and plasmids are listed in Supplemental Table S2 and Table S3, respectively. PrimeStar DNA polymerase for gene amplification was purchased from TaKaRa Biotech (Dalian, China), and 2 × Taq Master Mix polymerase for PCR verification and One Step Cloning Kit for plasmids construction were purchased from Vazyme Biotech (Nanjing, China). DNA gel purification and plasmid extraction kits were supplied by OMEGA Biotech (USA). All primers (Supplemental Table S4) were synthesized at Sangon Biotech (Shanghai, China). Yeast extracts, tryptone, agar powder, peptone and all other chemicals were from Sangon Biotech unless stated otherwise. All chemical standards were purchased from Sigma–Aldrich unless stated otherwise. The DMX analytical standard was synthesized by Yuanye Biotech (Shanghai, China). All codon optimized heterologous genes (Supplemental Table S5) were synthesized by Genewiz. *EfmvaS* (GenBank-KX064238) and *EfmvaE* (GenBank-KX064239) from *E. faecalis* were synthesized by Genewiz.

Genetic engineering

Gene knockout and integration were conducted by using a CRISPR/Cas9 system[60]. gRNA-expressing plasmids were constructed according to a previously described method[59]. The specific 20 bp sequence of the gRNA plasmid was designed by the CHOPCHOP webtool (http://chopchop.cbu.uib.no). All donor DNAs for gene deletion and integration were assembled by one-pot fusion PCR as previously described and then integrated into the corresponding genome loci[25]. The donor DNAs for gene knockout were prepared by fusing the upstream and downstream homologous arms.

The donor DNAs for genome integration were assembled by fusing promoters, target genes, terminators and homologous arms (Supplementary Fig. 9). *In situ* site-directed mutation of *ERG20* to $ERG20^{N127W}$ was conducted according to a previous method[59]. The mutated $ARO4^{K229L}$, $ARO7^{G141S}$ and $HMG2^{K6R}$ genes were performed by target mutation PCR. The promoter of *ACC1* (from -547 bp to -1 bp) was replaced with P_{TEF1}. The promoter of $ERG20^{N127W}$ (from-563 bp to -1 bp) was replaced with P_{HXT1} or P_{ERG1}.

For enzyme screening, PTase genes and truncated versions (Supplementary Fig. 2) from different organisms were codon-optimized for *S. cerevisiae* and then cloned into pESC-URA with *BamHI*/*HindIII* digestion. The $ScCHK$+IPK_{Sc}+$HlPT1L_{\Delta1\text{-}86}$ and $EfmvaE_{per}$+$ERG12_{per}$+$EfmvaS_{per}$+$HlPT1L_{\Delta1\text{-}86per}$ fragments were also assembled into pESC-URA and the constructed plasmids were named pESC-IUP and pESC-per, respectively. The *IDI1*-$HlPT1L_{\Delta1\text{-}86}$ and *CHIL2*-$HlPT1L_{\Delta1\text{-}86}$ fusions were assembled by using a $(GGGS)_3$ linker. Peroxisomal targeting of proteins was ensured by C-terminal addition of peroxisomal signal with the flexible linker GGGS. All transformants of *S. cerevisiae* were verified by colony PCR and DNA sequencing.

Strain cultivation

Transformation of *E. coli* was performed according to a previously described protocol [61]. Unless otherwise specified, *E. coli* strains were grown in Luria-Bertani (LB) medium (10 g/L tryptone, 5 g/L yeast extract, 10 g/L NaCl) at 37 °C and 220 rpm (Zhichu Shaker ZQZY-CS8). In addition, 100 mg/L ampicillin was normally supplemented for plasmid maintenance. Yeast strains were generally cultivated in YPD media consisting of 20 g/L peptone, 10 g/L yeast extract and 20 g/L glucose. Strains containing *URA3* based plasmids were selected on synthetic complete media without uracil (SD-URA), which consisted of 6.7 g/L yeast nitrogen base (YNB) without amino acids and 20 g/L glucose. The *URA3* marker was removed on SD+5FOA plates containing 6.7 g/L YNB, 20 g/L glucose and 1 g/L 5-fluoroorotic acid (5-FOA). Shake flask batch fermentations were conducted in 100 mL shake flasks with 20 mL of minimal medium (Delft-D) containing 2.5 g/L $(NH_4)_2SO_4$, 14.4 g/L KH_2PO_4, 0.5 g/L $MgSO_4 \cdot 7H_2O$, 20 g/L glucose, and trace metal and vitamin solutions[62]. All the above media were supplemented with 40 mg/L

histidine and/or 60 mg/L uracil if needed. Then, 20 g/L agar was added to make solid media. The yeast cells were cultivated at 30 °C and 220 rpm in liquid media for 96 h (Zhichu Shaker ZQZY-CS8) with an initial inoculation OD_{600} of 0.2.

Product extraction and quantification

For the extraction of xanthohumol and DMX, a low temperature, ultra-high pressure continuous flow cell disrupter was used to disrupt the yeast cells. Ten milliliters of culture broth from shake flask batch fermentation were cyclically broken three times at 1800 MPa. Then, 2 mL of each treated cell culture was added to an equal volume of ethyl acetate and vortexed thoroughly at 1600 rpm for 15 min. The ethyl acetate phase was collected, dried and resuspended in methanol. Before analysis, the extract solution was filtered through a 0.2-μm organic membrane. All extracted samples were quantified by high-performance liquid chromatography (HPLC). Samples were analyzed with a Poroshell 120 EC-C18 column (2.7 μm, 3 × 100 mm, Agilent) on a 1260 infinity II HPLC (Agilent) equipped with a photodiode array detector. Samples were eluted by a gradient method with two solvents: 0.05% formic acid (A) and acetonitrile with 0.05% formic acid (B). The gradient elution conditions were set as follows: 0-10 min, a linear gradient from 20% B to 55% B; 10-20 min, a linear gradient from 55% B to 65% B; 20-23 min, a linear gradient from 65% B to 90% B; 23-24 min, 90% B; 24-26 min, a linear gradient from 90% B to 20% B; then the system was equilibrated using the initial conditions (20% B) for 5 min before the next sample injection. The flow rate was 0.30 mL/min. The target products *p*-CA and N were detected by measuring the absorbance at 288 nm. DMX and xanthohumol were detected by measuring the absorbance at 370 nm. An Agilent 1290 Infinity II UHPLC system coupled to a 6470A triple quadrupole mass spectrometer and a ThermoFisher Q Exactive Hybrid Quadrupole-Orbitrap Mass Spectrometer in positive heated electrospray ionization mode was used quantitatively analyze xanthohumol.

Author contributions

S.Y. and Y.J.Z. conceived the study. S.Y. designed and performed most of the

experiments. R.C. contributed to strain construction. X.C. analyzed the data and revised the manuscript. G.W. contributed exogenous genes and analyzed the data. S.Y. and Y.J.Z. wrote the manuscript.

References

1. Kubeš, J. Geography of World Hop Production 1990–2019. *J. Am. Soc. Brew. Chem.* **80**, 84-91 (2022).
2. Xu, H. et al. Characterization of the formation of branched short-chain fatty acid:CoAs for bitter acid biosynthesis in hop glandular trichomes. *Mol. Plant.* **6**, 1301-1317 (2013).
3. Stevens, J.F. & Page, J.E. Xanthohumol and related prenylflavonoids from hops and beer: To your good health! *Phytochemistry* **65**, 1317-1330 (2004).
4. Miyata, S., Inoue, J., Shimizu, M. & Sato, R. Xanthohumol Improves Diet-induced Obesity and Fatty Liver by Suppressing Sterol Regulatory Element-binding Protein (SREBP) Activation. *J. Biol. Chem.* **290**, 20565-20579 (2015).
5. Miranda, C.L. et al. Antioxidant and prooxidant actions of prenylated and nonprenylated chalcones and flavanones in vitro. *J. Agric. Food Chem.* **48**, 3876-3884 (2000).
6. Legette, L. et al. Human pharmacokinetics of xanthohumol, an antihyperglycemic flavonoid from hops. *Mol. Nutr. Food Res.* **58**, 248-255 (2014).
7. Yong, W.K. & Abd Malek, S.N. Xanthohumol induces growth inhibition and apoptosis in ca ski human cervical cancer cells. *Evid. Based. Complement. Alternat. Med.* **2015** (2015).
8. Liu, M. et al. Pharmacological profile of xanthohumol, a prenylated flavonoid from hops (*Humulus lupulus*). *Molecules* **20**, 754-779 (2015).
9. Amoriello, T., Mellara, F., Galli, V., Amoriello, M. & Ciccoritti, R. Technological properties and consumer acceptability of bakery products enriched with brewers' spent grains. *Foods* **9**, 1492 (2020).
10. Chen, Q.-h. et al. Preparative isolation and purification of xanthohumol from hops (Humulus lupulus L.) by high-speed counter-current chromatography. *Food. Chem.* **132**, 619-623 (2012).
11. Grudniewska, A. & Popłoński, J. Simple and green method for the extraction of xanthohumol from spent hops using deep eutectic solvents. *Sep. Purif. Technol.* **250**, 117196 (2020).
12. Keasling, J.D. Manufacturing molecules through metabolic engineering. *Science (New York, N.Y.)* **330**, 1355-1358 (2010).
13. Li, S.J., Li, Y.R. & Smolke, C.D. Strategies for microbial synthesis of high-value phytochemicals. *Nat. Chem.* **10**, 395-404 (2018).
14. Galanie, S., Thodey, K., Trenchard, I.J., Interrante, M.F. & Smolke, C.D. Complete biosynthesis of opioids in yeast. *Science (New York, N.Y.)* **349**, 1095-1100 (2015).
15. Paddon, C.J. et al. High-level semi-synthetic production of the potent antimalarial artemisinin. *Nature* **496**, 528-532 (2013).
16. Liu, X. et al. Engineering yeast for the production of breviscapine by genomic analysis and synthetic biology approaches. *Nat. Commun.* **9**, 448 (2018).
17. Denby, C.M. et al. Industrial brewing yeast engineered for the production of primary flavor determinants in hopped beer. *Nat. Commun.* **9**, 965 (2018).
18. Facchini, P.J. et al. Synthetic biosystems for the production of high-value plant metabolites. *Trends. Biotechnol.* **30**, 127-131 (2012).

19. Thodey, K., Galanie, S. & Smolke, C.D. A microbial biomanufacturing platform for natural and semisynthetic opioids. *Nat. Chem. Biol.* **10**, 837-844 (2014).
20. Brown, S., Clastre, M., Courdavault, V. & O'Connor, S.E. De novo production of the plant-derived alkaloid strictosidine in yeast. *Proc. Natl Acad. Sci. USA* **112**, 3205-3210 (2015).
21. Ban, Z. et al. Noncatalytic chalcone isomerase-fold proteins in *Humulus lupulus* are auxiliary components in prenylated flavonoid biosynthesis. *Proc. Natl Acad. Sci. USA* **115**, E5223-E5232 (2018).
22. Li, H. et al. A heteromeric membrane-bound prenyltransferase complex from hop catalyzes three sequential aromatic prenylations in the bitter acid pathway. *Plant. Physiol.* **167**, 650-659 (2015).
23. Nagel, J. et al. EST analysis of hop glandular trichomes identifies an O-methyltransferase that catalyzes the biosynthesis of xanthohumol. *Plant Cell* **20**, 186-200 (2008).
24. Novák, P., Matoušek, J. & Bříza, J. Valerophenone synthase-like chalcone synthase homologues in *Humulus lupulus*. *Biol. Plant.* **46**, 375-381 (2003).
25. Zhou, Y.J. et al. Modular pathway engineering of diterpenoid synthases and the mevalonic acid pathway for miltiradiene production. *J. Am. Chem. Soc.* **134**, 3234-3241 (2012).
26. Jendresen, C.B. et al. Highly active and specific tyrosine ammonia-Lyases from diverse origins enable enhanced production of aromatic compounds in bacteria and *Saccharomyces cerevisiae*. *Appl. Environ. Microbiol.* **81**, 4458-4476 (2015).
27. Abe, I., Morita, H., Nomura, A. & Noguchi, H. Substrate Specificity of Chalcone Synthase: Enzymatic Formation of Unnatural Polyketides from Synthetic Cinnamoyl-CoA Analogues. *J. Am. Chem. Soc.* **122**, 11242-11243 (2000).
28. Rodriguez, A., Kildegaard, K.R., Li, M., Borodina, I. & Nielsen, J. Establishment of a yeast platform strain for production of *p*-coumaric acid through metabolic engineering of aromatic amino acid biosynthesis. *Metab. Eng.* **31**, 181-188 (2015).
29. Zhou, Y.J. et al. Production of fatty acid-derived oleochemicals and biofuels by synthetic yeast cell factories. *Nat. Commun.* **7**, 11709 (2016).
30. Ignea, C., Pontini, M., Maffei, M.E., Makris, A.M. & Kampranis, S.C. Engineering monoterpene production in yeast using a synthetic dominant negative geranyl diphosphate synthase. *ACS. Synth. Biol.* **3**, 298-306 (2014).
31. Martinez-Munoz, G.A. & Kane, P. Vacuolar and plasma membrane proton pumps collaborate to achieve cytosolic pH homeostasis in yeast. *J. Biol. Chem.* **283**, 20309-20319 (2008).
32. Tsurumaru, Y. et al. An aromatic prenyltransferase-like gene *HlPT-1* preferentially expressed in lupulin glands of hop. *Plant. Biotechnol.* **27**, 199–204 (2010).
33. Wang, R. et al. Molecular characterization and phylogenetic analysis of two novel regio-specific flavonoid prenyltransferases from *Morus alba* and *Cudrania tricuspidata*. *J. Biol. Chem.* **289**, 35815-35825 (2014).
34. Li, J. et al. Biocatalytic access to diverse prenylflavonoids by combining a regiospecific *C*-prenyltransferase and a stereospecific chalcone isomerase. *Acta Pharm. Sin. B* **8**, 678-686 (2018).
35. Sasaki, K., Tsurumaru, Y., Yamamoto, H. & Yazaki, K. Molecular characterization of a membrane-bound prenyltransferase specific for isoflavone from *Sophora flavescens*. *J. Biol. Chem.* **286**, 24125-24134 (2011).
36. Chen, R. et al. Regio- and stereospecific prenylation of flavonoids by *Sophora flavescens* prenyltransferase. *Adv. Synth. Catal.* **355**, 1817-1828 (2013).

37. Shen, G. et al. Characterization of an isoflavonoid-specific prenyltransferase from *Lupinus albus*. *Plant. Physiol.* **159**, 70-80 (2012).
38. Yang, T. et al. Stilbenoid prenyltransferases define key steps in the diversification of peanut phytoalexins. *J. Biol. Chem.* **293**, 28-46 (2018).
39. He, J. et al. Regio-specific prenylation of pterocarpans by a membrane-bound prenyltransferase from *Psoralea corylifolia*. *Org. Biomol. Chem.* **16**, 6760-6766 (2018).
40. Rea, K.A. et al. Biosynthesis of cannflavins A and B from *Cannabis sativa L*. *Phytochemistry* **164**, 162-171 (2019).
41. Luo, X. et al. Complete biosynthesis of cannabinoids and their unnatural analogues in yeast. *Nature* **567**, 123-126 (2019).
42. Qian, S., Clomburg, J.M. & Gonzalez, R. Engineering *Escherichia coli* as a platform for the in vivo synthesis of prenylated aromatics. *Biotechnol. Bioeng.* **116**, 1116-1127 (2019).
43. Xie, W., Ye, L., Lv, X., Xu, H. & Yu, H. Sequential control of biosynthetic pathways for balanced utilization of metabolic intermediates in *Saccharomyces cerevisiae*. *Metab. Eng.* **28**, 8-18 (2015).
44. Ignea, C. et al. Orthogonal monoterpenoid biosynthesis in yeast constructed on an isomeric substrate. *Nat. Commun.* **10**, 3799 (2019).
45. Chen, R. et al. Engineering cofactor supply and recycling to drive phenolic acid biosynthesis in yeast. *Nat. Chem. Biol.* **18**, 520-529 (2022).
46. Cao, X. et al. Engineering yeast for high-level production of diterpenoid sclareol. *Metab. Eng.* **75**, 19-28 (2022).
47. Chatzivasileiou, A.O., Ward, V., Edgar, S.M. & Stephanopoulos, G. Two-step pathway for isoprenoid synthesis. *Proc. Natl Acad. Sci. USA* **116**, 506-511 (2019).
48. Dahl, R.H. et al. Engineering dynamic pathway regulation using stress-response promoters. *Nat. Biotechnol.* **31**, 1039-1046 (2013).
49. Yuan, J. & Ching, C.-B. Dynamic control of ERG9 expression for improved amorpha-4,11-diene production in *Saccharomyces cerevisiae*. *Microb. Cell. Fact.* **14**, 38 (2015).
50. Hammer, S.K. & Avalos, J.L. Harnessing yeast organelles for metabolic engineering. *Nat. Chem. Biol.* **13**, 823-832 (2017).
51. Cao, X., Yang, S., Cao, C. & Zhou, Y.J. Harnessing sub-organelle metabolism for biosynthesis of isoprenoids in yeast. *Synth. Syst. Biotechnol.* **5**, 179-186 (2020).
52. Dusseaux, S., Wajn, W.T., Liu, Y., Ignea, C. & Kampranis, S.C. Transforming yeast peroxisomes into microfactories for the efficient production of high-value isoprenoids. *Proc. Natl. Acad. Sci. U S A* **117**, 31789-31799 (2020).
53. Peng, B. et al. A squalene synthase protein degradation method for improved sesquiterpene production in Saccharomyces cerevisiae. *Metab. Eng.* **39**, 209-219 (2017).
54. Guo, X. et al. Enabling Heterologous Synthesis of Lupulones in the Yeast *Saccharomyces cerevisiae*. *Appl. Biochem. Biotechnol.* **188**, 787-797 (2019).
55. Levisson, M. et al. Toward Developing a Yeast Cell Factory for the Production of Prenylated Flavonoids. *J. Agric. Food. Chem.* (2019).
56. Munakata, R. et al. Isolation of Artemisia capillaris membrane-bound di-prenyltransferase for phenylpropanoids and redesign of artepillin C in yeast. *Commun. Biol.* **2**, 384 (2019).
57. Wang, P. et al. Complete biosynthesis of the potential medicine icaritin by engineered *Saccharomyces cerevisiae* and *Escherichia coli*. *Sci. Bull.* **66**, 1906-1916 (2021).
58. Chen, R. et al. Molecular insights into the enzyme promiscuity of an aromatic prenyltransferase.

Nat. Chem. Biol. **13**, 226-234 (2017).
59. Yang, S., Cao, X., Yu, W., Li, S. & Zhou, Y.J. Efficient targeted mutation of genomic essential genes in yeast *Saccharomyces cerevisiae*. *Appl. Microbiol. Biotechnol.* **104**, 3037-3047 (2020).
60. Mans, R. et al. CRISPR/Cas9: a molecular Swiss army knife for simultaneous introduction of multiple genetic modifications in *Saccharomyces cerevisiae*. *FEMS. Yeast. Res.* **15** (2015).
61. Inoue, H., Nojima, H. & Okayama, H. High efficiency transformation of *Escherichia coli* with plasmids. *Gene* **96**, 23-28 (1990).
62. Verduyn, C., Postma, E., Scheffers, W.A. & Van Dijken, J.P. Effect of benzoic acid on metabolic fluxes in yeasts: a continuous-culture study on the regulation of respiration and alcoholic fermentation. *Yeast* **8**, 501-517 (1992).

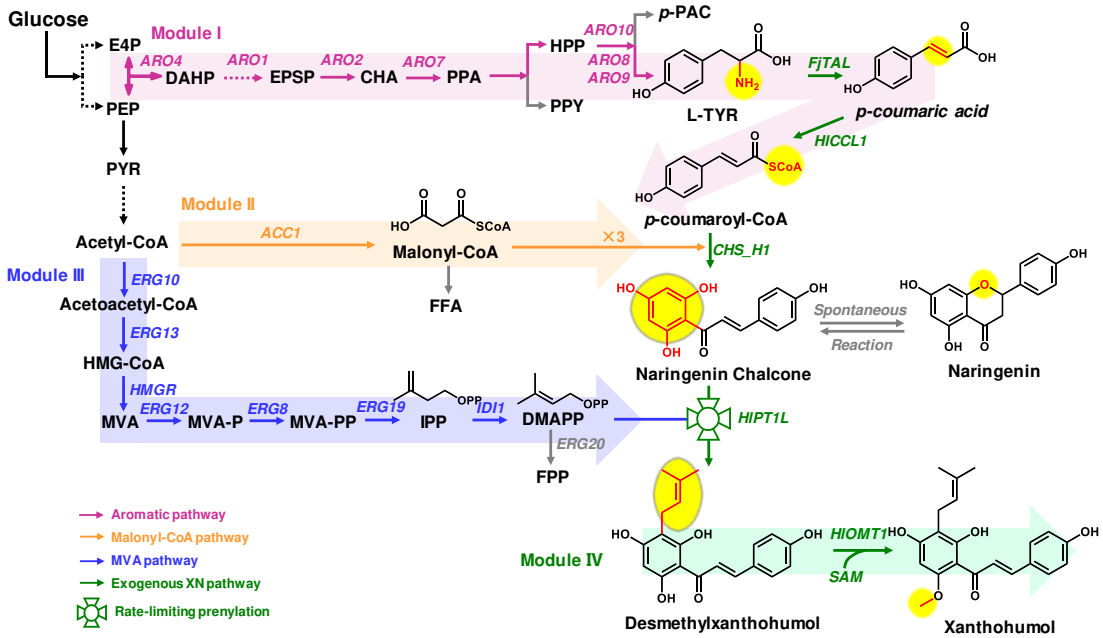

Fig. 1 Engineered metabolic pathway for the *de novo* biosynthesis of xanthohumol in yeast. The DMX biosynthetic pathway was derived from three endogenous module pathways, including the aromatic pathway (Module I, purple label), malonyl-CoA pathway (Module II, orange label), and MVA pathway (Module III, blue label). Then, DMX was methylated to form xanthohumol (Module IV, green label). Exogenous enzymes are also labeled in green and competing metabolic pathways are labeled in gray. Dotted arrows represent multiple steps. E4P, erythrose 4-phosphate; PEP, phosphoenolpyruvate; DAHP, 3-deoxy-D-arabino-heptulosonic acid 7-phosphate; EPSP, 5-enolpyruvyl-shikimate-3-phosphate; CHA, chorismic acid; PPA, prephenate; PPY, phenylpyruvate; HPP, para-hydroxy-phenylpyruvate; *p*-PAC, para-hydroxy-acetaldehyde; L-TYR, L-tyrosine; FFA, free fatty acid; PYR, pyruvate; HMG-CoA, 3-hydroxy-3-methylglutaryl coenzyme A; MVA, mevalonate; MVA-P, mevalonate-5-phosphate; MVA-PP, mevalonate-5-pyrophosphate; DMAPP, dimethylallyl diphosphate; IPP, isopentenyl pyrophosphate; FPP, farnesyl pyrophosphate.

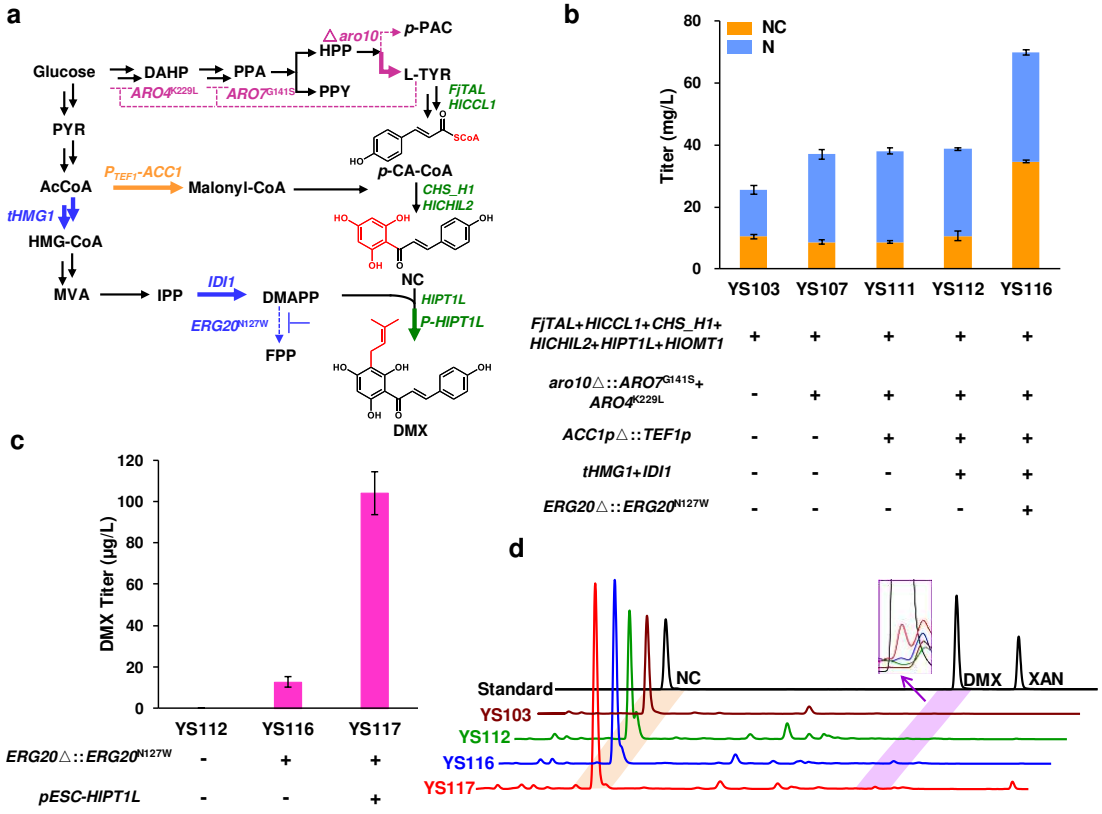

Fig. 2 Optimizing the DMX *de novo* biosynthetic pathway. a, Schematic overview of the modification of three metabolic modules. Upregulated steps are indicated with bold arrows, and downregulated or knockout steps are shown with dashed arrows. FjTAL, tyrosine ammonia-lyase; HlCCL1, 4-coumarate-coenzyme A ligase; CHS_H1, chalcone synthase; HlCHIL2, noncatalytic chalcone isomerase; HlPT1L, prenyltransferase; aro10, phenylpyruvate decarboxylase; ARO4^{K229L} and ARO7^{G141S}, resistant versions of DAHP synthase and chorismate mutase; ACC1, acetyl-CoA carboxylase; tHMG1, truncated HMG-CoA reductase 1; IDI1, isopentenyl diphosphate isomerase; ERG20^{N127W}, variant of farnesyl diphosphate synthase; P-HlPT1L, overexpression of prenyltransferase by the pESC-*URA* plasmid. b, Metabolic modification of these three modules improved the production of the precursors NC/N. c, Mutation of *ERG20* and overexpression of *HlPT1L* improved DMX production. d, HPLC analysis of the DMX standard and the fermented product of strains YS103, YS112, YS116 and YS117. All data are presented as the mean ± s.d. of three yeast clones.

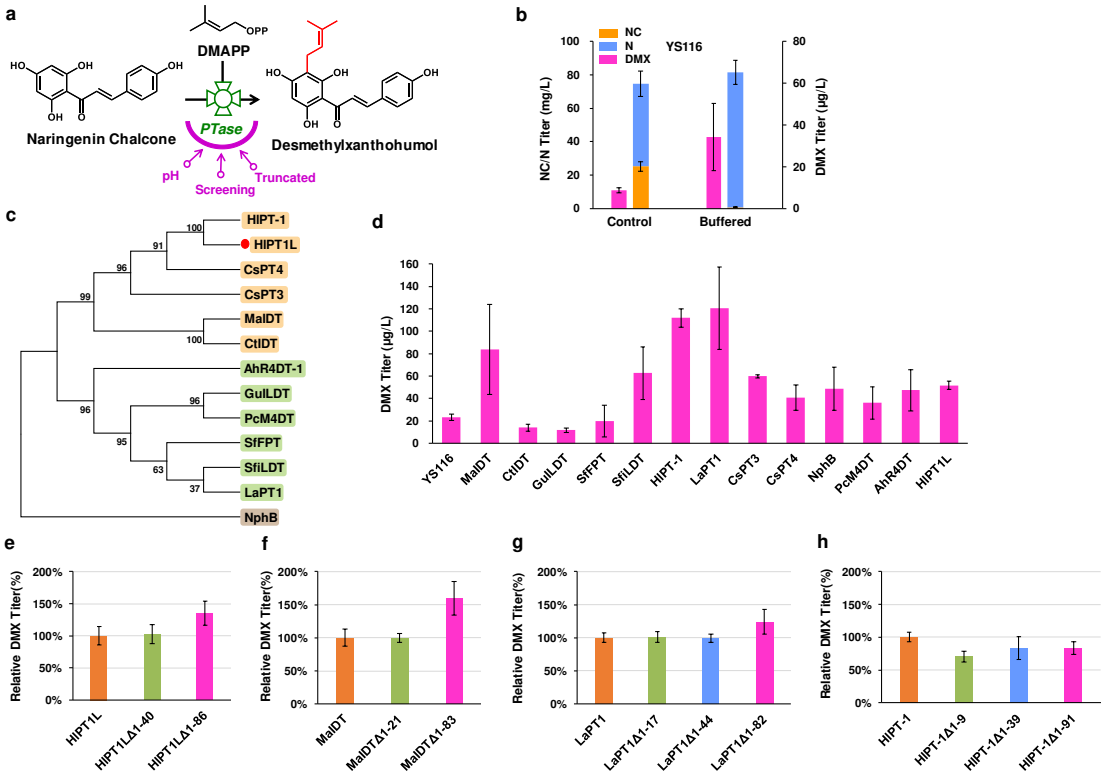

Fig. 3 Engineering the PTase to enhance DMX production. a, Schematic illustration of PTase engineering. To improve the catalytic ability of PTase by changing the pH, we characterized the alternative PTase and truncated the signal peptides. b, Adding MES buffer solution increased DMX production in strain YS116. MES buffer with a pH value of 6.58 was added after 24 h of fermentation. c, Phylogenetic analysis of PTases. A neighbor-joining tree was constructed by using MEGA7 software and a maximum likelihood method with 1000 bootstrap tests. d. Evaluating different PTases in strain YS116 by using high-copy plasmids. e-h, Truncating PTases for DMX production in strain YS116. All data are presented as the mean ± s.d. of three yeast clones.

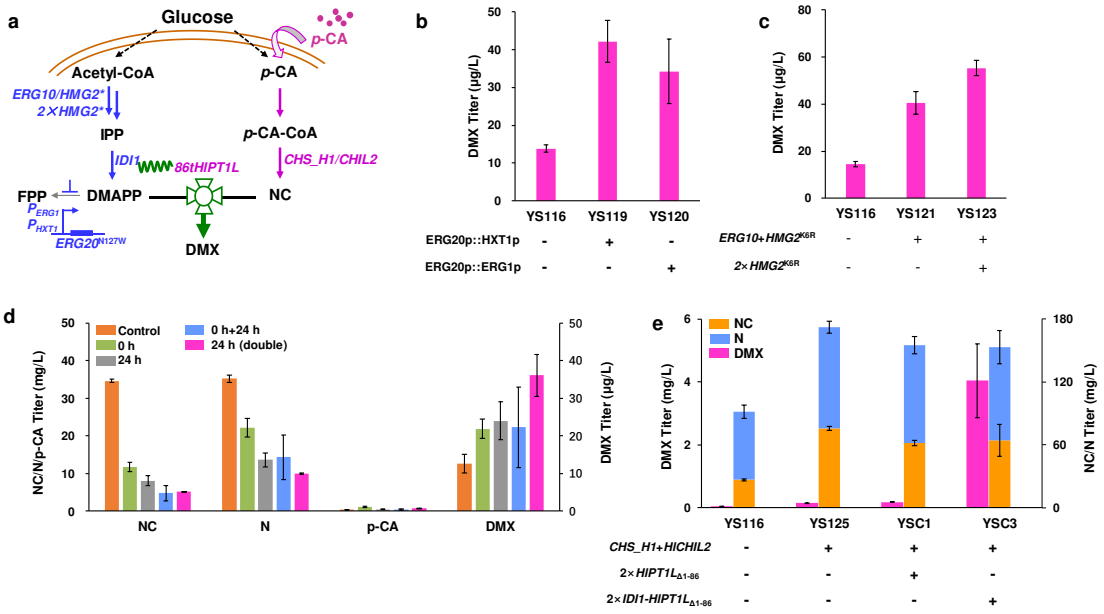

Fig. 4 Engineering substrate supply and channeling to enhance DMX production. a, Schematic diagram of substrate supply and channeling. Enzyme overexpression is shown in purple and blue, and downregulated expression is indicated in gray. The supply of DMAPP was increased by overexpressing *ERG10* and *HMG2*^{K6R} and replacing the native promoter of *ERG20*^{N127W} with the promoter P_{HXT1} or P_{ERG1}. The supply of NC was enhanced by feeding *p*-CA or overexpressing *CHS_H1* and *HlCHIL2*. *IDI1-HlPT1L*$_{\Delta 1\text{-}83}$ fusion with the linker $(GGGS)_3$ enhanced substrate channeling. b, Replacing the native promoter of *ERG20*^{N127W} with the promoter P_{HXT1} or P_{ERG1} improved DMX production. c, Overexpression of *ERG10* and *HMG2*^{K6R} increased DMX production. d, Addition of *p*-CA at different times to produce DMX. For 0 h and 24 h, 140 mg/L *p*-CA was added at 0 h and 24 h, respectively. For 0 h + 24 h, 140 mg/L *p*-CA was added at both 0 h and 24 h. For 24 h (double), 280 mg/L *p*-CA was added at 24 h. e, Overexpression of *CHS_H1*, *HlCHIL2* or *IDI1-HlPT1L*$_{\Delta 1\text{-}83}$ fusion increased DMX production. All data are presented as the mean ± s.d. of three yeast clones.

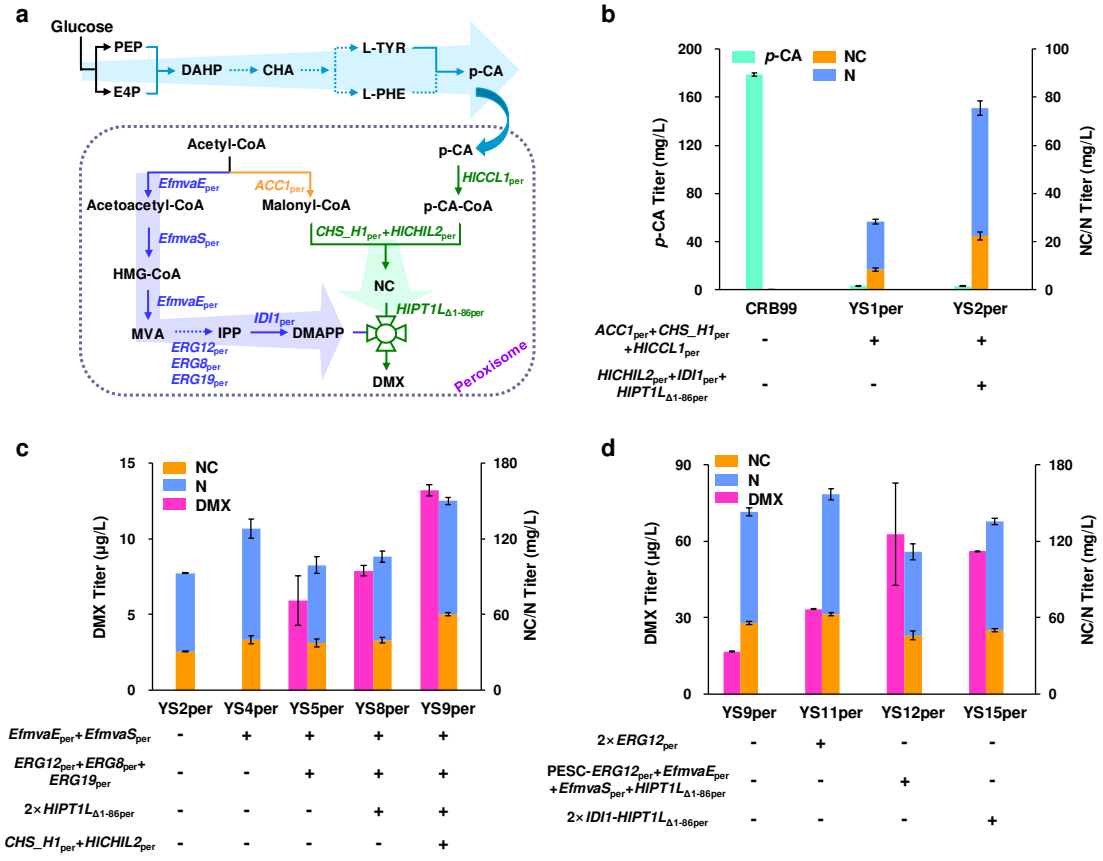

Fig. 5 Engineering DMX biosynthesis in peroxisomes. a, Overview of the engineered metabolic pathway for DMX biosynthesis in peroxisomes. Precursor *p*-CA was efficiently produced in the cytosol. The 3-step reaction from *p*-CA to DMX was targeted to the peroxisome in the *p*-CA overproducing chassis RB99. The malonyl-CoA and MVA pathway modules were also targeted to the peroxisomes. *EfmvaE*$_{per}$, *E. faecalis* acetoacetyl-CoA thiolase/HMG-CoA reductase; *EfmvaS*$_{per}$, *E. faecalis* HMG-CoA synthase; ERG12$_{per}$, mevalonate kinase; *ERG8*$_{per}$, phosphomevalonate kinase; *ERG19*$_{per}$, mevalonate diphosphate decarboxylase; *IDI1*$_{per}$, isopentenyl diphosphate isomerase; *ACC1*$_{per}$, acetyl-CoA carboxylase; *HlCCL1*$_{per}$, 4-coumarate-coenzyme A ligase; *CHS_H1*$_{per}$, chalcone synthase; *HlCHIL2*$_{per}$, noncatalytic chalcone isomerase; *HlPT1L*$_{\Delta1\text{-}86per}$, truncated PTase. b, Engineering peroxisomal malonyl-CoA and DMX biosynthetic modules for synthesis of the precursor NC/N. c, Construction of the complete MVA pathway in the peroxisome enabled *de novo* synthesis of DMX and increased DMX production by enhancing PTase expression and NC supply. d, Optimizing the MVA pathway and overexpressing *IDI1-HlPT1L*$_{\Delta1\text{-}86per}$ increased DMX production. All data are presented as the mean ± s.d. of three yeast clones.

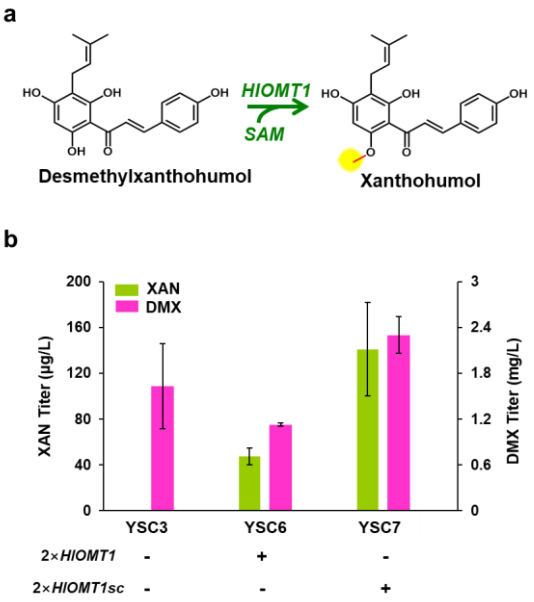

Fig. 6 *De novo* biosynthesis of xanthohumol. a, Scheme of xanthohumol production from DMX by an O-methyltransferase (HlOMT1). b, Overexpressing *HlOMT*1 and *HlOMT1*sc (codon-optimized for *S. cerevisiae*) for xanthohumol (XAN) production. All data are presented as the mean ± s.d. of three yeast clones.

Supplementary Files

This is a list of supplementary files associated with this preprint. Click to download.

- SupplementaryMaterials.pdf
- 22890.pdf